Journal of Physics: Conference Series

PAPER • OPEN ACCESS

Real-time, upstream, radiotherapy verification using a Monolithic Active Pixel Sensor System

To cite this article: J J Velthuis *et al* 2020 *J. Phys.: Conf. Ser.* **1662** 012034

Real-time, upstream, radiotherapy verification using a Monolithic Active Pixel Sensor System

J J Velthuis[1,2,3], L Beck[1], R Hugtenburg[1,2,4], J Pritchard[1] and C de Sio[1]
[1]School of Physics, University of Bristol, Bristol, BS7 1TL, United Kingdom
[2]Swansea University Medical School, Singleton Park, Swansea, SA2 8PP, United Kingdom
[3]School of Nuclear Science and Technology, University of South China, No 28 West Changsheng Rd, Hengyang, China
[4]Department of Medical Physics and Clinical Engineering, Abertawe Bro Morgannwg University Hospital Board, Swansea SA2 4QA

E-mail: Jaap.Velthuis@bris.ac.uk

Abstract. Intensity modulated radiotherapy is a widely used technique for accurately targeting cancerous tumours in difficult locations. As treatments are becoming more complex, new methods need to be developed to monitor them. Monolithic active pixel sensors are a viable candidate for providing upstream beam monitoring during treatment. A MAPS based system can be made thin enough to have less than 1% attenuation. We have already demonstrated leaf position resolutions below 130μm at the iso-centre for 5mm wide leaves sampled 34 times per second. We have shown that the signal due to therapeutic photons can be determined and thus the dose in patient. Furthermore, the sensor works well inside an MR-linac, allowing leaf position verification even in that challenging environment.

1. Introduction

The introduction of advanced high-precision radiotherapy, coupled with more hypofractionated treatments requires the dose to be delivered more accurately. Volumetric Modulated Arc Therapy (VMAT) means the linear accelerator treatment machine (linac) continuously reshapes the radiation beam as it moves around the body using a multileaf collimator system (MLC) to closely fit the area of the tumour. The MLC consists of two opposing rows of tungsten leaves, in which the individual leaves move independently of each other, allowing for complex field shapes to be created during treatment delivery. To maintain total dose errors below 2% for complex treatments, the positions of the leaves need to be verified to 300μm precision [1]. Incorporating a high precision, real time treatment monitoring device would allow systematic and random MLC errors to be identified instantaneously and subsequently addressed. Several approaches exist. They can broadly be divided in three categories: checking of log files, downstream and upstream monitoring. Checking of logfiles, see for example [2], is technically not verification as leaf motors might be stuck but still return the correct location or the MLC is misaligned, nor is it performed in real time [3]. In downstream monitoring the beam profile is measured after traversing the patient, see for example [4]. This is very difficult as the patient forms a very complex scatter centre. In upstream monitoring, the beam is measured before entering the patient. The key challenge here is to keep the attenuation low, ideally less than 1%, to prevent beam hardening, which changes the beams energy spectrum and reduces the depth at which

the maximum treatment dose is absorbed and increases the skin dose. A Monolithic Active Pixel Sensor based system is an ideal candidate for an upstream monitoring system [5, 6].

2. Monolithic Active Pixel Sensors

A MAPS consists of a three layer structure: on top of a highly p-type doped substrate a lower p-type doped silicon, the epitaxial layer, is grown and on top of that, in a highly p-doped layer, an n-well and an amplifier is integrated, see figure 1. When a charged particle traverses the sensor, electron-hole pairs are generated. The electrons generated in the epitaxial layer are confined to that layer due to the built-in potential. The electrons diffuse through the epitaxial layer until they reach the depleted zone underneath the diode. Here the electrons are collected. The top layer that houses the transistors is less than a micron thick. The first couple of microns of the substrate layer are needed to create the built-in potential difference. The rest is only used for mechanical support. The epitaxial layer, the layer where signal generation takes place, is typically between ~2 and ~20μm thick. Hence the device can be made less than 30μm thick without loss of signal-to-noise by thinning the device from the back. This means that the beam would pass through the sensor undisturbed (<0.1% attenuation).

In this work we use the Lassena [7], a 12×14cm^2, 3-side buttable, 3T sensor with 50μm pitch. This allows to tile large areas in a 2×N configuration without significant dead space in between. A 2×2 matrix of these sensors covers a large enough area to be clinically deployed. The sensor reads out frames at a rate of 34 frames per second.

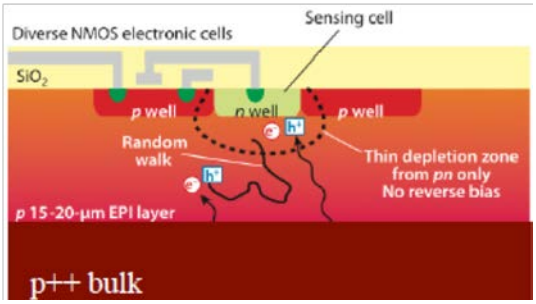

Figure 1. Cross section of a MAPS. Radiation will generate electron hole pairs. The electrons are collected at the *n*-well.

3. Leaf position reconstruction

For treatment verification in radiotherapy it is essential to determine the location of the leaves with great precision in very short time segments. With a different sensor, the Achilles [8] which measures ~6×6cm^2 and has 15 μm pitch, we demonstrated a leaf edge resolution of 52±4μm at the isocentre using 0.1 s of data taken at 400 Mu/min for static fields for leaves with a width of 1cm at isocentre [9]. The algorithm used is based on a Sobel filter. Leaf misplacements as small as 0.5mm were detected and moving leaves were tracked [10].

To improve the performance, we moved to a Fully Convolutional Neural Network (FCNN) Multi-Task model to automatically detect the leaf and infer its position. This was performed on images taken with the Lassena sensor. The “r-UNet" model is inspired by UNet [11], with the addition of Fully Connected layers to perform the position estimation. The dataset used for training consisted of 900 frames for each of 10 considered leaf positions. The leaves used here are 5mm wide at the isocentre. The leaf extensions ranged between 1 and 35mm. Six positions were used for training, and the remaining four are used to test the performance of the trained model. Of the training dataset, 80% was used for training and validation and the remaining 20% was used for tests. The Loss Function used to optimise the learning is a combination of the Dice Loss coefficient for the leaf detection, and of mean squared error (MSE) for the leaf position estimation. The combined loss is defined as: Loss = ($\boldsymbol{\alpha}$ × Dice Loss) + (1-$\boldsymbol{\alpha}$) × MSE. For $\boldsymbol{\alpha}$=0.6, an average dice loss coefficient of 0.85±0.03m with an average MSE of 0.02mm was obtained for the images in the test set. Applying the model to unseen leaf positions yielded single-leaf resolutions between 60 and 130μm, see figure 2, depending on the

leaf extension. This is much better than the required 300μm resolution. Note that the positions are determined 34 times per second, so this allows proper real time verification.

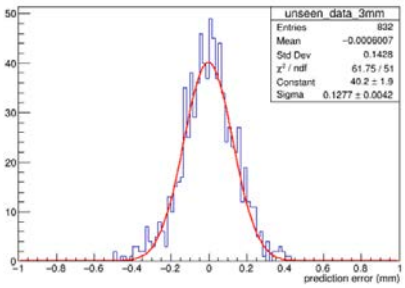

Figure 2. Distribution of predicted errors for unseen data for 3mm extension yielding a resolution of 127±4μm.

4. Dosimetry using MAPS

To extract the dose in patient, the number of photons traversing the detector needs to be determined. This is challenging as the signal measured in the MAPS is the result of both the interactions of therapeutic photons and the interactions of the background electrons with the MAPS. This is indicated in figure 3. The therapeutic photons can produce electrons inside the epitaxial layer of the MAPS by Compton scattering of the photon in the epitaxial layer, see process 1 and 2. Compton scattering in air, in the accelerator or in the top layer (non-sensitive) of the MAPS, see process 3 and 4, and pair production yield contamination electrons that result in an additional signal.

A simple way to measure the number of photons in the beam is to exploit the Compton scattering in the non-sensitive part of the sensor, see process 4. The number of these Compton electrons can be manipulated by patterning the sensor. When the blocks are kept relatively thin, the signals of all processes in figure 3 are the same throughout the detector except for process 4. By subtracting the total signal directly underneath a low bit from the total signal directly underneath a high bit, the signal due to the interactions of the therapeutic photons with the extra amount of silicon is measured. This technique only relies on the knowledge of the amount of extra material. Given the precision with which these microstructures can be produced, the number of photons can be extracted with high precision [12]. Figure 4 shows a profile perpendicular to the structure. The modulation can be clearly observed, demonstrating that the patterning indeed leads to a modulation of the signal that can be precisely measured and thus the dose in patient can be extracted using this technique. Optimisation measurements on the size and depth of the patterning are under way.

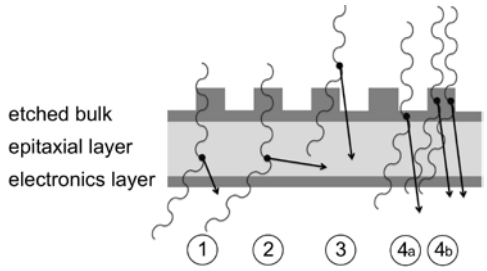

Figure 3. Compton scattering of a photon in the epitaxial layer (1, 2), in the air/LINAC (3), and in the grating etched in the bulk (4).

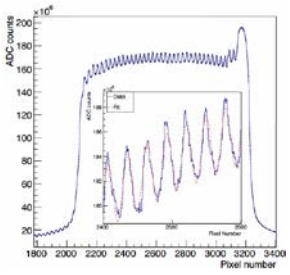

Figure 4. Profile of signal response perpendicular to the gratings. Inset: Fitted data for a 7×7 field.

5. Operation in MR-linac

With the advent of the combination MRI-LINAC [13] there are additional challenges associated with treatment verification, in particular the influence of the magnetic field on detector and in-patient dosimetry. Conventional strategies may not be applicable. As the epilayer in MAPS is very thin

compared to the radius of the eddy loops the charge carriers will perform in the magnetic field, they can operate in high magnetic fields without significant signal loss. An Achilles sensor was placed inside the bore of a prototype MR-linac, which combined a 1.5 T Phillips MRI scanner and a 6MV Elekta linear accelerator. Data was taken at 400MU/min with 1mm of RW3 solid water and a 2mm air gap for several square fields. A signal profile for the different field sizes along a row of pixels can be seen in figure 5. Instead of observing the expected top hat signal shape, the electrons generated in the solid water and the sensor are moving towards the left due to the magnetic field. This generates the observed shape. The rising and falling edges can be parametrized by an exponential fall or rise. The time constants are all the same within errors independent of the field size, as expected since the shape will depend in the magnetic field strength and the electron momentum spectrum. These results show that the system can be used in an MR-linac for leaf position verification.

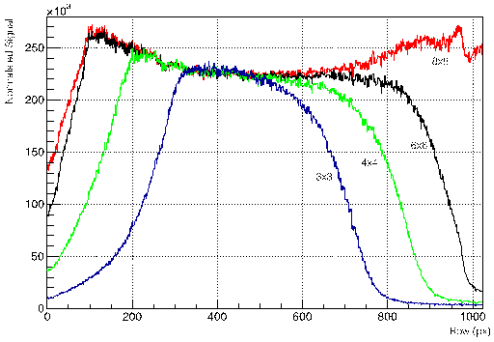

Figure 5. Normalised profiles of the beam along a row of pixels measured with 1mm build up in an MR-linac. Please note that the sensor only measures 6×6cm^2, hence the characteristic falling edge on the righthand side for the 8×8 field falls outside the measurable area.

6. Conclusions

We are developing a MAPS based system for upstream beam monitoring during treatment. A MAPS based system can be made thin enough to have less than 1% attenuation. We have already demonstrated leaf position resolutions below 130µm at the iso-centre for 5mm wide leaves measured 34 times per second. We have shown that the signal due to therapeutic photons can be determined by patterning the sensor and thus the dose in patient can be extracted. Furthermore, we have shown that the sensor operates well in the magnetic field of an MR-linac enabling leaf position verification in these advanced therapies. All this combined shows that MAPS are an excellent candidate to realise novel, real-time upstream monitoring devices.

7. References

[1] Agarwal A *et al* 2019 *J. Radiother. Prac.* Sept 225-31
[2] Agnew A *et al* 2014 *Phys. Med. Biol.* **59** N49-63
[3] Vial P *et al* 2006 *Phys. Med. Biol.* **51** 5517-38
[4] Celi S *et al* 2016 *J. Appl. Clin. Med. Phys.* **17** 262-76
[5] Velthuis J *et al* 2018 *EU Patent* EP2654895B1
[6] Velthuis J *et al* 2016 *US Patent* US9,517,358 b2
[7] Sedgwick I *et al* 2013 *Proceedings International Image Sensor Workshop* Utah, USA 297-300
[8] Guerrini N *et al* 2011 *J. Instrument.* **6** C03003
[9] Page R *et al* 2013 Nucl. *Instrum. Meth. Phys. Res. A* **731** 295-8
[10] Beck L *et al* 2019 *Appl. Rad. Isotop.* **156** 108951
[11] Ronneberger O *et al* 2015 *MICCAI Lecture Notes in Computer Science* **9351** Springer
[12] Velthuis J *et al* 2020 International Application No PCT/GB2018/050583
[13] Raaymakers B W *et al* 2009 *Phys. Med. Biol.* **54** N229-37